

# Numerical Simulation of Aeroacoustics of Hovering Helicopter Rotor

A N Kusyumov<sup>1</sup>, S A Mikhailov<sup>1</sup>, S A Kusyumov<sup>1</sup>, K V Fayzullin<sup>1</sup> and G N Barakos<sup>2</sup>

<sup>1</sup>Department of Aerohydrodynamics, KNRTU-KAI, 10 K. Marx str., Kazan, 420111, Russia

<sup>2</sup>James Watt South Building, School of Engineering, University of Glasgow, G12 8QQ, Scotland

postbox7@mail.ru

**Abstract.** The specifics of the problem of estimating the noise of a hovering rotor, allows for some simplification of the Ffowcs Williams-Hawkins (FW-H) equation. Most published works dedicated to helicopter tonal noise estimates use the far-field formulation. This paper estimates the aeroacoustic emissions of a helicopter rotor in hover, for observers placed at different distances using the FW-H equation, including near-field and far-field terms. The blade pressure distribution is obtained from numerical simulations with the RANS equations. To demonstrate this approach, the near- and far-field contributions are analyzed for the model-scale UH-1H main helicopter rotor. For the numerical simulations, the HMB solver of Glasgow University and the ANSYS Fluent13 commercial solver are used. As the rotor blade behaviour is characterized by a complex motion in the computer program it is assumed that the blade is seen in as a rotating rigid body. The most commonly used mathematical model of the FW-H equation corresponds to the classical impermeable formulation. In this case, the source surface corresponds to the blade surface. Then, the acoustic pressure (based on the FW-H 1A formulation) is modified with empirical adjustments, based on the radiation Mach number. This was applied for the near- or far-field thickness noise depending on the rotor-observer distance.

## 1. Introduction

The prediction of aircraft noise falls in the area of Computational Aeroacoustics (CAA). CAA combines flow data obtained by Computational Fluid Dynamics (CFD) for a region near the aircraft surface, and wave propagation equations, to estimate the aircraft noise far away from their sources.

For a conventional helicopter, there are two main components contributing to the generation of near- and far-field noise, the main rotor and the tail rotor [1]. The helicopter main rotor generates tonal and broadband noise. The tonal noise in hover is dominant in a conical region directed 30 to 40 degrees downwards of the rotor plane, while broad-band noise radiates mostly out of the plane of the rotor. Most of works on helicopter rotor noise employ the Ffowcs Williams-Hawkins (FW-H) equation [2]. This equation separates the noise in thickness and loading noise components, and its general formulation allows for estimates of the acoustic emissions for observers in the near- and far-field of the rotor.



Both thickness and loading noise components can be presented as a sum of several terms, what are functions of the distance between the rotor and the observers. The nature of the dependence of noise components on the rotor-observer distance determines the near- and far-field terms. It allows for simplification of the FW-H equation for different observer locations. Most published works dedicated to helicopter tonal noise estimation use the far-field formulation (see, for example, references [3, 4]). Typically, the far-field formulation is applied to the Mach-scaled rotors. In the case of low blade tip Mach number the direct CFD simulation can be used for the near-field noise estimation, based on Reynolds-Averaged Navier-Stokes (RANS) equation (see reference [5]). Due to the limited space of wind tunnels, comparisons with experimental measurements require the complete formulation of the FW-H equation, including the near- and far-field terms.

This paper estimates the aeroacoustics of the UH-1H model-scale, helicopter rotor [6] in hover, for different observer distances. The acoustic pressure is determined via the FW-H equation. The far-field FW-H equation solution is compared to experimental reference data. And the contributions of the different FW-H equation components for different rotor-observer distances are analyzed. For the numerical modelling, the HMB solver of Glasgow University and ANSYS Fluent13 are used.

## 2. FW-H equation

The general retarded-time formulation of Farassat, for the observer aeroacoustic pressure  $p'$  is commonly referred to as Formulation 1A [2] and is given by the following expression:

$$p'(x, t) = p'_T(x, t) + p'_L(x, t), \quad (1)$$

where  $p'_T(x, t)$  and  $p'_L(x, t)$  are the thickness and load noise respectively. For an arbitrary rotor-observer distance the thickness and load noise components can be written as

$$p'_T(x, t) = p'_{TN}(x, t) + p'_{TF}(x, t), \quad p'_L(x, t) = p'_{LN}(x, t) + p'_{LF}(x, t). \quad (2)$$

The subscripts  $N$  and  $F$  stand for the near- and far-field terms defined by

$$p'_{TF}(x, t) = \frac{1}{4\pi} \int_{f=0} \left[ \frac{\rho_0 \dot{v}_n}{r|1=M_r|^2} + \frac{\rho_0 v_n \hat{r}_i \dot{M}_i}{r|1=M_r|^3} \right]_{ret} dS, \quad (3)$$

$$p'_{TN}(x, t) = \frac{1}{4\pi} \int_{f=0} \left[ \frac{\rho_0 a_0 v_n (M_r - M^2)}{r^2 |1=M_r|^3} \right]_{ret} dS, \quad (4)$$

$$p'_{LF}(x, t) = \frac{1}{4\pi a_0} \int_{f=0} \left[ \frac{\dot{p} \cos(\theta)}{r|1=M_r|^2} + \frac{p \cos(\theta) \hat{r}_i \dot{M}_i}{r|1=M_r|^3} \right]_{ret} dS, \quad (5)$$

$$p'_{LN}(x, t) = \frac{1}{4\pi} \int_{f=0} \left[ \frac{p(\cos(\theta) - M_i n_i)}{r^2 |1=M_r|^2} + \frac{p \cos(\theta) (M_r - M^2)}{r^2 |1=M_r|^3} \right]_{ret} dS. \quad (6)$$

Here  $p$  is the pressure at emission point;  $a_0$  is the speed of sound;  $M_r = M_i \hat{r}_i$  is the Mach number of source in radiation direction;  $r = |\mathbf{x} - \mathbf{y}|$  is the distance between observer and source,  $\mathbf{x}$  is the observer position vector, and  $\mathbf{y}$  is the source position vector. The above expressions also include  $\cos(\theta) = \mathbf{n} \cdot \hat{\mathbf{r}}$ , with  $\theta$  the local angle between the normal vector  $\mathbf{n}$  to the emission surface, and the radiation direction  $\hat{\mathbf{r}}$  at the time of emission. A dot over variables is used as a symbol of differentiation with respect to the time of the emission source. The subscript *ret* stands for the retarded time with the integration evaluated over the emission surface. For solution of the FW-H equation numerical (CFD) simulation results are used for the acoustic pressure at source.

The mathematical model (1)–(6), corresponds to the classical impermeable formulation of FW-H equations. In this case, the source surface  $f=0$  corresponds to the blade surface. This model, for high blade tip Mach numbers, usually gives under predicted values of the noise level. Nevertheless the classical FW-H formulation was used in recent publications for relatively low values of the blade tip Mach numbers (see reference [7], for example). Then, the acoustic pressure (based on the Formulation 1A) can be modified with empirical adjustments, based on the radiation Mach number  $M_r$ . In the present paper the radiation vector  $\hat{\mathbf{r}}$  of the source – observer distance projected to shaft – observer direction is used instead of the source-observer distance. This was applied for the near- or far-field thickness noise depending on the rotor-observer distance.

The employed algorithm is similar to the algorithm, described in [3]. The first stage of FW-H solution algorithm is to divide the rotor blade surface in a number of panels. Integration over each panel is approximated using the value at its centroid.

The algorithm was implemented to the in-house H-FWH computer code.

### 3. CFD Modelling

The numerical simulations were conducted for 1/7 scaled UH-1H rotor; the geometry of the full-scale UH-1H rotor is presented in table 1. Since temporal and spatial periodicity is assumed for the flow, the computational grid was constructed for a single rotor blade (with appropriate periodic boundary conditions). For this two-bladed rotor, the computational domain is a half of a cylinder. The multi-block topology used in this paper, can be seen in Figure 1. C-type blocking is used around the blade. The structured and multi-block computational grid consisted of 88 blocks and 8.4 million cells. Along the aerofoil surface 218 points are located with concentration near the leading and trailing edges. Normal to the surface the first cell size is  $10^{-5}$  of the blade's chord length and the cell aspect ratio is less than 1.2.

**Table 1.** UH-1H operational characteristics

Parameter	Value
Number of blades $N$	2
Rotor diameter $2R$ , m	14.63
Rotor solidity $\sigma$	0.0464
Blade chord $c$ , m	0.53
Blade airfoil	NACA 0012
Blade twist (root to tip), deg	-10.9
Max gross weight $W$ , $N$	43000

The multi-block topology used in this work, can be seen in Figure 1. Around the blade a C-topology is used.

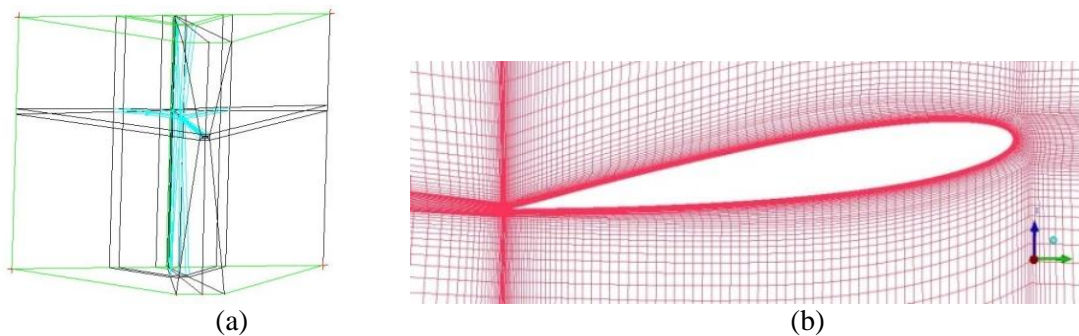


**Figure 1.** Multi-block topology (a) and mesh section (b).

The flow fields were numerically simulated using the 3D steady RANS equations.

For HMB the “source-sink” boundary conditions [8] were used at all surfaces of the computational domain apart from the symmetry plane. The “periodic” boundary condition provides the periodicity of the flow around the blade. The inflow ( $W_{in}$ ) and outflow ( $W_{out}$ ) velocities were obtained from momentum theory according to the expressions:

$$W_{in}(x, y, z_u) = -\frac{U}{8}\sqrt{C_T}\left(\frac{R}{L}\right)^2; W_{out} = -U\sqrt{C_T}. \quad (7)$$

Here  $U$  is the speed of the blade tip;  $L$  is the distance between the rotor centre and an arbitrary  $(x, y, z_u)$  point on the upper surface  $z_u = \text{const}$  of the computational domain. The thrust coefficient  $C_T$  is determined as

$$C_T = \frac{T}{\pi R^2 q_{tip}}, \quad (8)$$

where  $q_{tip}$  is the dynamic pressure at the blade tip and  $T$  is the rotor thrust, obtained after iterative computations. The rotor thrust coefficient  $C_{TW}$  (under the condition  $T=W$ ) is first used as an initial guess and then the thrust coefficient value  $C_T$  is recomputed using successive approximations.

Similar boundary conditions with some differences at the bottom part of modeling domain were used for the HMB and Fluent solvers: in Fluent for the bottom part of computational domain the «pressure-outlet» boundary condition was assigned.

The flow conditions, and the values of the trust coefficient obtained with HMB and Fluent are presented in table 2. A collective pitch angle  $\theta_{0.75}$  was chosen according to approximate trimming methods [9]. The values  $\bar{W}_{in}$  of averaged on the upper part of the computational domain used for computations in both HMB and Fluent are shown in table 2. Some discrepancy between HMB and Fluent results can be explained, by the different type of boundary conditions at the upper and bottom parts of the computational domain: in Fluent  $W_{in} = \bar{W}_{in} = const$ , and for the bottom part of computational domain the «pressure-outlet» boundary condition was assigned.

**Table 2.** Conditions for computations

Parameter	Value
Collective pitch, $\theta_{0.75}$	7 °
Tip Mach number, $M_{tip}$	0.8
Tip Reynolds number, Re	$9.5 \times 10^6$
Thrust coefficient (for $T=W$ ), $C_{TW}$	0.0055
Inflow velocity (HMB), $\bar{W}_{in}$	0.201 m/s
Inflow velocity (Fluent), $\bar{W}_{in}$	0.2 m/s
Thrust coefficient (HMB), $C_T$	0.00577
Thrust coefficient (Fluent), $C_T$	0.0054

Simulations were conducted with the  $k-\omega$  SST turbulence model. Results for the surface pressure coefficient distribution are show in Figure 2.

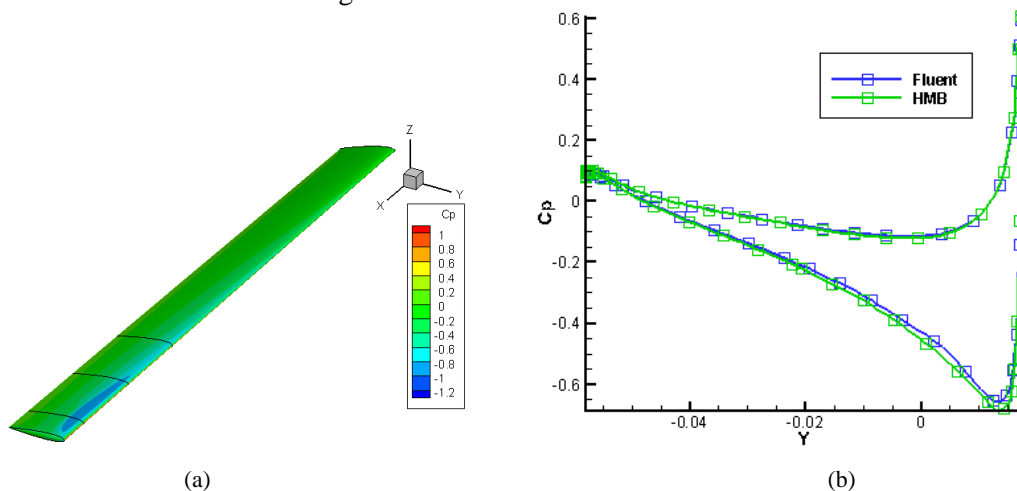


**Figure 2.** Distribution of the pressure coefficient  $C_p$ : on the UH-1H rotor blade surface (a), and at the blade section  $\bar{r} = r/R = 0.75$  (b).

The pressure distribution at the observer plane section is shown in Figure 3.

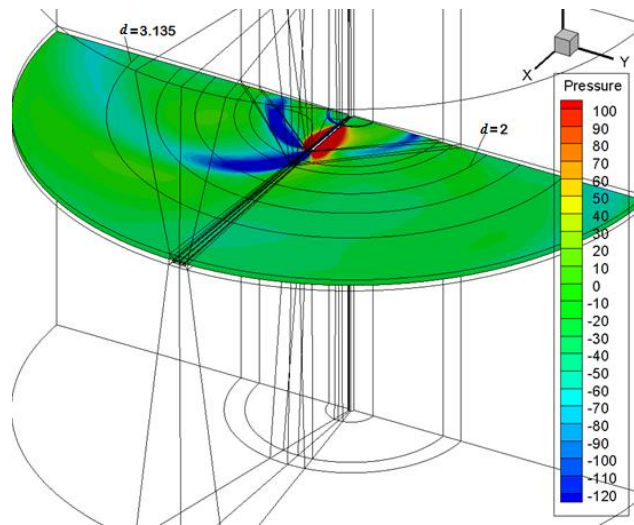


**Figure 3.** Absolute pressure distribution at the observer plane section.

From Figure 3 it follows that the obtained CFD simulation results for the near-field area (distance between the rotor center and the observer  $d < 2R \approx 2$  m) allows for comparison of the aeroacoustic signal at the CFD post processing stage (denoted as “direct” evaluation, without any further processing) to the FW-H equation solution results. At the distance  $d > 2.5R$  comparison of the “direct” evaluation of the CFD results to the FW-H equation solution results can be not correct because of poor grid resolution in the far-field area.

#### 4. FW-H equation solutions

Figure 4 presents the results of numerical simulation and experiments [6] for a far-field observer located at the rotor disc plane on the distance of  $3R=3.135$  m (see Figure 3) away of the rotor.

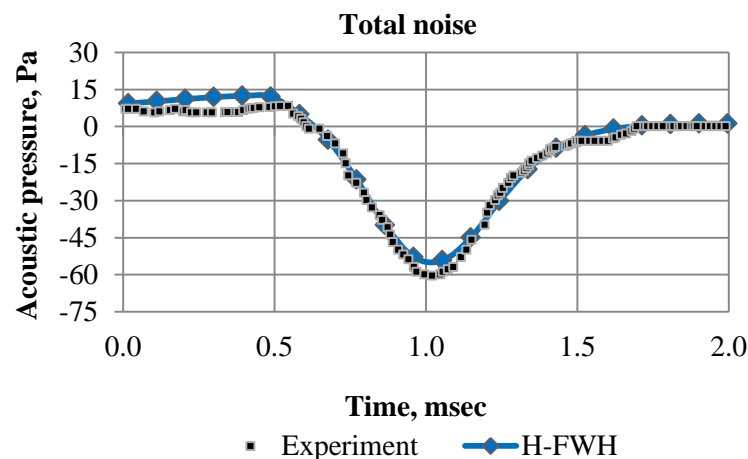


**Figure 4.** Comparison of CFD and experimental data for a far-field observer at  $3R$  on the rotor disk plane.

The total noise predicted by the H-FWH code for an observer located in the rotor plane is in good agreement with the measurements. Comparison of the computed FW-H peak values to theoretical asymptotes

$$p'_{Fmin}(d) = p'_{min}(3R) \frac{3R}{d}, \quad p'_{Nmin}(d) = p'_{min}(3R) \left(\frac{3R}{d}\right)^2 \quad (9)$$

is presented in Figure 5.

The expressions (9) provide approximations of the limited peak values for observers located in the near- and far-field areas. The difference between the FW-H peak and the  $P'_{Nmin}$  values corresponds to the contribution of the near-field terms of the FW-H equation that were omitted in this analysis.

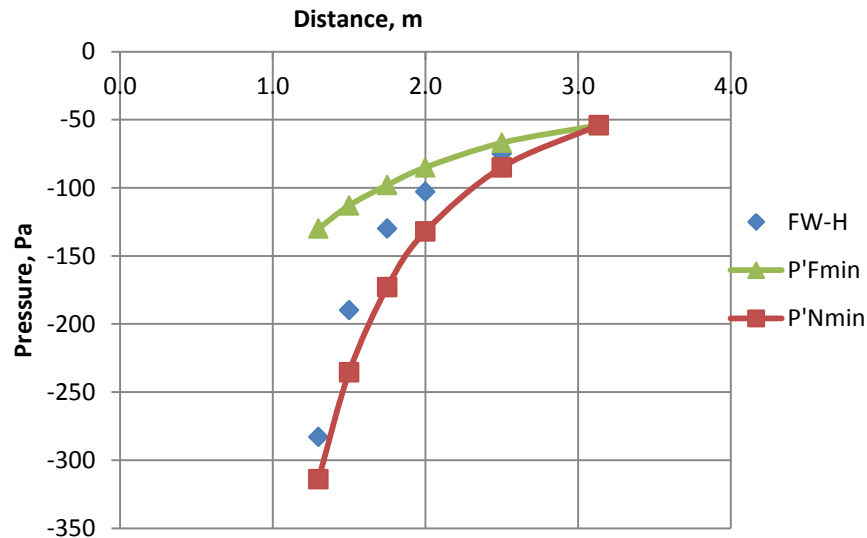


**Figure 5.** Comparison approximate and FW-H peak values.

From Figure 5 it follows that for short rotor-observer distances ( $d \ll R$ ) computation of the near-field terms of the system (1)–(6) is important.

## 5. Conclusions

Application of the in-house code for the FW–H (Ffowcs Williams – Hawkins) numerical solution was considered for near-field observers. The total rotor noise was calculated as a sum of the thickness and load noise including the near- and far-field components. To determine the near-field flow parameters for the UH–1H rotor in hover mode, the CFD code is used. Comparison of the computed FW-H peak values to theoretical asymptotes shows that computation of the near-field terms for short rotor-observer distances is important for accurate predictions of the observer noise.

## Acknowledgements

This work was supported by the grant No. 9.1577.2017/4.6 of the Ministry of Education and Science of the Russian Federation.

## References

- [1] Edwards Band Cox Ch 2002 *NASA/CR-2002-211650*.
- [2] Ffowcs Williams J E, Hawkins D L 1969 *Philosophical Transactions of the Royal Society A* **264** (1151) pp 321–343
- [3] Brentner K S, Farassat F 2003 *Progress in Aerospace Sciences* **39** pp 83–120
- [4] Song Wen-ping, Han Zhong-hua, Qiao Zhi-de 2006 *25th International Congress of the Aeronautical Sciences ICAS* pp 1–9
- [5] Stepanov R, Pakhov V, Bozhenko A, Batrakov A, Garipova L, Kusyumov A, Mikhailov S, Barakos G *International Journal of Aeroacoustics* 2017 vol 16 issue 6 pp 460–475
- [6] Shmitz F H and Yu Y H 1983 *NASA Technical memorandum* 84390 p 105
- [7] Sharma K, Brentner K *AHS 72nd Annual Forum* 2016 pp 1–14
- [8] Mohd N A, Barakos G N, *RAeS Aerodynamics Conference* 2010 pp 1–19
- [9] Seddon J *Basic helicopter aerodynamics* 1990 (BSP professional books) p 137